
This is an electronic reprint of the original article.
This reprint may differ from the original in pagination and typographic detail.

Lestinsky, P.; Väyrynen, Petri; Vecer, M.; Wichterle, K.

Hydrodynamics of airlift reactor with internal circulation loop

Published in:

20th International Congress of Chemical and Process Engineering CHISA 2012 25 – 29 August 2012, Prague, Czech Republic

DOI:

[10.1016/j.proeng.2012.07.482](https://doi.org/10.1016/j.proeng.2012.07.482)

Published: 01/01/2012

Document Version

Publisher's PDF, also known as Version of record

Published under the following license:

CC BY-NC-ND

Please cite the original version:

Lestinsky, P., Väyrynen, P., Vecer, M., & Wichterle, K. (2012). Hydrodynamics of airlift reactor with internal circulation loop: Experiment vs. CFD simulation. In *20th International Congress of Chemical and Process Engineering CHISA 2012 25 – 29 August 2012, Prague, Czech Republic* (pp. 892-907). (Procedia Engineering; Vol. 42). Elsevier. <https://doi.org/10.1016/j.proeng.2012.07.482>

This material is protected by copyright and other intellectual property rights, and duplication or sale of all or part of any of the repository collections is not permitted, except that material may be duplicated by you for your research use or educational purposes in electronic or print form. You must obtain permission for any other use. Electronic or print copies may not be offered, whether for sale or otherwise to anyone who is not an authorised user.

20th International Congress of Chemical and Process Engineering CHISA 2012
25 – 29 August 2012, Prague, Czech Republic

Hydrodynamics of airlift reactor with internal circulation loop: Experiment vs. CFD simulation

P. Lestinsky a*, P. Vayrynen^b, M. Vecer^a, K. Wichterle^a

^aDept. of Chemistry, VSB-Technical University of Ostrava 17. listopadu 15, Ostrava 70833, Czech Republic

^bDept. of Material Science and Engineering School of Chemical Technology, Aalto University, Vuorimiehentie 2, Espoo, Finland

Abstract

Effect of geometrical parameters on two phase hydrodynamics of airlift reactor is the main topic of present paper. Laboratory scale apparatus with internal circulation loop consists of concentric draft tube, in which a gas bubbles rising. Setup of draft tube inside of reactor is important geometry parameter and has big influence on two phase hydrodynamics. In experiment was studied influence of changes diameter of draft tube to hydrodynamics in airlift reactor. Results of experiments (liquid velocity and gas hold-up) were compared with the simple CFD simulations performed in COMSOL Multiphysics 3.5a. For each point of gas volumetric flow in simulation, were determined conditions of bubble diameter and bubble drag coefficient. Although bubble break-up and coalescence were neglected, the results of numerical simulation are in pretty good agreement with experimental data.

© 2012 Published by Elsevier Ltd. Selection under responsibility of the Congress Scientific Committee (Petr Kluson) Open access under [CC BY-NC-ND license](https://creativecommons.org/licenses/by-nc-nd/4.0/).

Keywords: Bubbles; airlift reactor; draft tube; CFD simulation

* Corresponding author. Tel.: +420 597 324 230;
E-mail address: pavel.lestinsky@vsb.cz .

Nomenclature

A_g	cross-section area to gas input (m^2)
C_μ	turbulence modeling constant, $C_\mu = 0.09$ (1)
$C_{\phi 1}$	turbulence modeling constant, $C_{\phi 1} = 1.44$ (1)
$C_{\phi 2}$	turbulence modeling constant, $C_{\phi 2} = 1.92$ (1)
C_k	bubble induced turbulence modeling constant, $C_k = 0.01 - 1$ (1)
C_ϕ	bubble induced turbulence modeling constant, $C_\phi = 1 - 1.9$ (1)
c_D	drag coefficient (1)
d_b	bubble diameter (m)
F	volume force (interaction force) (N/m^3)
g	gravity acceleration, $g = 9.81$ (m^2/s)
$\Delta h_{r,d}$	difference of level in reverse U-tube manometer in riser and downcomer (m)
$K_{B,T}$	loss coefficient at the bottom and at the top (1)
M	molecular weight of gas, $M_{air} = 0.029$ (kg/mol)
N_p	gas mass flux ($kg/(m^2 \text{ s})$)
Δp	pressure difference (Pa)
p	hydrostatic pressure (Pa)
Q_g	input gas volumetric flow (m^3)
R	universal gas constant, $R = 8.314$ ($J/(mol.K)$)
S_k	additional source term ($kg/(m^3.s)$)
T	temperature of liquid, $T = 288$ (K)
u_l	liquid velocity (m/s)
U_l	superficial liquid velocity (m/s)
u_g	gas velocity (m/s)
U_g	superficial gas velocity (m/s)
u_{slip}	slip velocity (m/s)
$\Delta z_{r,d}$	difference of height between delivery point from reverse U-tube manometer in riser and downcomer (m)
ϕ	dissipation rate of turbulent energy (m/s^3)
ϵ_g	gas hold-up (1)
$\epsilon_{gr,gd}$	gas hold-up in riser and downcomer (1)
ϵ_l	liquid hold-up (1)
η_l	viscosity of liquid (Pa.s)

η_T	turbulent viscosity (Pa.s)
ρ_g	density of gas (kg/m^3)
ρ_D	density of gas-liquid dispersion (kg/m^3)
ρ_l	density of liquid (kg/m^3)
k	kinetic energy (m^2/s^2)
σ_k	turbulence modeling constant, $\sigma_k = 1$ (1)
σ_ϕ	turbulence modeling constant, $\sigma_\phi = 1.3$ (1)
ξ	loss coefficient (1)

1. Introduction

The Airlift reactors are finding increasing applications in chemical industry, biochemical fermentation and biological wastewater treatment processes [1,2]. Generally there are two types of airlift reactors: reactor with internal and with external circulation loop.

For design of an airlift reactor with internal circulation loop, it is necessary to have accurate estimates of the phase hold-ups and velocity in the riser and in the downcomer. Several literature studies have focused on the estimation of these hydrodynamics parameters [3-5]. The velocities of the liquid in the downcomer and in the riser are dependent on the frictional losses, which are determined by geometry of the airlift reactor and operating condition.

Several recent publications have established the potential of CFD simulation for describing the hydrodynamics of airlift reactors [6-9].

1.1. Airlift reactor

The upward flowing liquid in the center of the column can be stabilized over the whole height by inserting a draft tube. This type of column is called a bubble column loop reactor. Bubble columns loops are commonly known as Airlift reactors. Air is injected through a sparger at or near the bottom of the up-flow section, the so called riser. The reduced density of the two phase mixture in the riser causes a circulation in the loop in the same way as with an air-lift pump. High gas flow rates are possible. Airlift reactors are widely used in process industries in recent years because of the following advantages: simple construction without moving parts, good mass heat transfer characteristics, efficient mixing with low energy consumption, and simple operation with low cost [10].

1.2. Bubble flow model

Essentially two basic approaches to simulation of flow dynamics of two-phase gas-liquid systems are known. The first is an approach where both the liquid phase and the gas-phase motion are considered as a homogeneous. These two-fluid approximations are presented in Eulerian representation and thus referred to as Euler-Euler simulation. The second approach treats only the liquid-phase motion in an Eulerian representation and computes the motion of the dispersed gas-phase elements in a Lagrangian way by individually tracking them on their way through the liquid body. This approach has been termed Euler-Lagrange representation.

Two fluids Euler-Euler model is basic macroscopic model for two-phase fluid flow. The derivation of the model equations for the two-phase bubbly flow starts with the assumption that both phases can be described as continua, governed by the partial differential equations of continuum mechanism. The phases are separated by an interface, which is assumed to be a surface. At the interface, jump condition for the conservation of mass and momentum can be formulated. Bubble flow is simplification of two-fluid flow model with following assumptions:

- density of gas is negligible compared with density of liquid
- motion of gas bubble relative to liquid is determined by balance between viscous shear and pressure force
- pressure field are equivalent for both phases

The sum of the momentum equation for both phases is result from these assumptions. The sum of equation content the momentum equation for liquid velocity, the continuity equation and the transport equation for gas hold-up.

The interaction between the various phases follows from the distribution of the pressure and shear stress at the interface. However, the details of these are not known and cannot be resolved in the Euler-Euler approach, as individual interfaces are not represented in this theoretical framework. Instead, the interaction forces have to be formulated separately and fed back to the momentum equation [11].

1.3. Interfacial forces

The magnitude of F describes the interaction force between the continuous and the dispersed phase. The plus marker is given for gas phase and the minus marker is given for liquid phase. Sokolichin [12,13] considered, that only the pressure and the gravity forces has been effect on stationary gas bubble in stationary liquid in two-phase flow. Since there is usually a relative motion between the bubble and the liquid, the liquid flow around individual bubbles leads to local variations in pressure and shear stress. Usually three different contributions for the interaction force term are taken into account, a friction force term $-F_f$, an inertia force term $-F_i$ and a lift force term $-F_l$, leading to the following approximation for the force of interaction:

$$F = F_f + F_i + F_l \quad (1)$$

The friction force is calculated by:

$$F_f = -\varepsilon_g C_w (u_g - u_l) \quad (2)$$

where C_w is friction coefficient. Schwarz [14] determined values of $C_w = 5.10^4 \text{ kg}/(\text{m}^3 \cdot \text{s})$ for $u_{slip} = 0,2 \text{ m/s}$.

The inertia force is given equation:

$$F_i = -\varepsilon_g C_i \rho_l d(u_g - u_l)/dt \quad (3)$$

where C_i is coefficient corresponding of amount of liquid, which is moved by gas bubble. Cook and Harlow [15] provided from experiment, that $C_i = 0,25$.

Last term in equation (15) is the lift force, which Thomas [16] express by relation:

$$F_l = -\varepsilon_g C_l \rho_l (u_g - u_l) \times (\nabla \times u_l) \quad (4)$$

where C_l is coefficient of buoyancy. Delnoij [17] provided this coefficient as $C_l = 0,53$. Boisson [18] suggested compound of friction force and inertia force together and replace them by the drag force. The drag force is calculated by relation:

$$F_D = 3/4 c_D/d_b \varepsilon_g \varepsilon_l \rho_l u_{slip} (u_g - u_l) \quad (5)$$

This approach (i.e. the drag force and the lift force were used for simulation) used another authors [19-21] and they has been good agreement numerical results with experimental data. On the other hand Joshi [22] used relation:

$$F_D = (\varepsilon_g (\rho_g - \rho_l) g (u_g - u_l))/(u_g - u_l) \quad (6)$$

On the basic of these examinations, Sokolichin [23] used for determined interfacial force only the lift force and the drag force. Without the lift force, the stationary bubbles hold in the stagnant liquid and without drag force, the bubbles has infinite acceleration.

The COMSOL Multiphysics 3.5a make it possible input of interfacial force F as a constant. The magnitude of the interfacial force has a great influence to the resulting liquid velocity and gas hold-up. The equation (6) was used for our simulation, because it does not contain a constant as drag coefficient and bubble diameter. These constants obtain equation of the slip velocity and we obtained the two

independent variables (slip velocity and interfacial force). In simulation we used the simplification of continuity equation; therefore we simplified equation (6) to term:

$$F_D = (\rho_g - \rho_l) g \quad (7)$$

The interfacial force after substitution of constants is:

$$F = -9778 \text{ N/m}^3 \quad (8)$$

Azzopardi [11] published a sum of interfacial forces occur between both phases. In our simulations we calculating with the simplification of continuity equation and many variables at interfacial forces is not necessary for us.

1.4. Slip velocity and drag coefficient

The slip velocity is name for relative velocity between gas and liquid phase. It is a one of the main parameters of multiphase flow. Together with interfacial force belong to variables, which could affect the result of numerical simulations. The slip velocity can be calculated as:

$$u_{slip} = -((4 d_b \Delta p)/(3 c_D \rho_l))^{0.5} \quad (9)$$

The most important parameters are the bubble diameter - d_b and the drag coefficient - c_D . Another parameters is the hydrostatic pressure - p , but his values cannot be affected. The bubble diameter is assumed as a constant (equivalent sphere diameter), over all reactor. This assumption has been used also by other authors [5,24]. In some cases of numerical simulations the bubble diameter was represented by a bubble size distribution. Khrisna [25] uses such approach for three-phase flow reactor with Fisher-Tropsh synthesis, when attention was focused on the kinetics and the mass transfer rate.

Bubble diameter in present numerical simulation follows paper by Johansen [26], who uses eq. (10) as bubble size diameter for case when gas is injected into the bottom part through orifice.

$$d_b = 0.35 (Qg^2/g)^{0.2} \quad (10)$$

Drag coefficient is another important parameter for slip velocity determination. There are many approaches how to determine the drag coefficient which has been published in literature. Clift [27] published beside standard drag curve for solid spherical particle also empirical lines denotes behaviour of drops and bubbles in contaminated and pure liquid systems. Graphical dependence of the drag coefficient vs. the Reynolds number can be seen in Fig. 1.

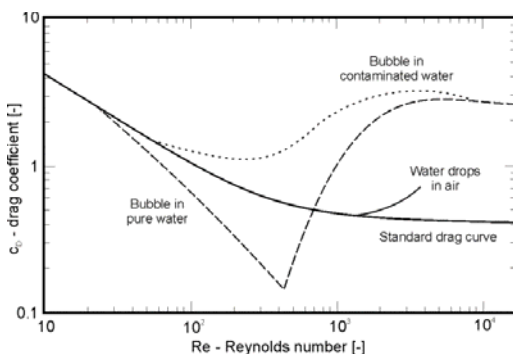


Fig. 1. Drag coefficient as a function of Reynolds number for water drops in air and air bubbles in water, compared with standard drag curve for rigid spheres

Schiller [28] made a correlation of the drag coefficient vs. the Reynolds number for spherical particles (11), (12).

$$0 < Re < 1000 \quad c_D = 24/Re (1 + 0.15 Re^{0.687}) \quad (11)$$

$$Re > 1000 \quad c_D = 0.44 \quad (12)$$

Delnoij [29] used this consideration for numerical simulation of bubble column reactor. Application of these equations is safe for bubbles with diameter smaller than 1 mm (spherical shape).

Empiric formula covering effect of surface tension was introduced by Johansen [26]. They used the Eötvös number for prediction of the drag coefficient for larger bubbles with non-spherical shapes:

$$c_D = 0.622/(1/E\ddot{o} + 0.235) \quad (13)$$

Ranade [30] and Bhanu [31] used this from for calculation of bubble drag coefficient in ultrapure water. The values of drag coefficient corresponding to the curve (13) are denoted as “bubble in pure water” (dashed line in Fig. 1) in the region of $Re > 1000$.

1.5. Numerical model

Nowadays, when supercomputer exists, the ways for simulation multiphase flow, counting individual movement and behavior of each bubble (break-up and coalescence, collision dynamics, oscillation of shape) are open. Unfortunately, no commercial software covers all of those processes and specific in-house codes are needed [32].

Anyway, using software such FLUENT or COMSOL for simulation of multiphase flows seems to be not much effective, but it can bring useful information. Simulation of internal loop airlift reactor under conditions similar with experiments was carried out using COMSOL. The governing equations calculated in this case were as follows:

The momentum equation for liquid phase:

$$\varepsilon_l \rho_l (\partial u_l / \partial t) + \varepsilon_l \rho_l u_l \nabla u_l = -\nabla p + \nabla [\varepsilon_l (\eta_l + \eta_T) (\nabla u_l + \nabla u_l^T)] + \varepsilon_l \rho_l g \pm F \quad (14)$$

where η_T is turbulent viscosity defined as:

$$\eta_T = \rho_l C_\mu k^2 / \varphi \quad (15)$$

where k is the turbulent kinetic energy, φ is the dissipation rate of turbulent energy and their values are calculated by closure equations:

$$\rho_l \partial k / \partial t - \nabla [(\eta + \eta_T / \sigma_k) \nabla k] + \rho_l u_l \nabla k = 1/2 \eta_T (\nabla u_l + \nabla u_l^T)^2 - \rho_l \varphi + S_k \quad (16)$$

$$\rho_l \partial \varphi / \partial t - \nabla [(\eta + \eta_T / \sigma_\varphi) \nabla \varphi] + \rho_l u_l \nabla \varphi = 1/2 C_{\varphi 1} \varphi / k \eta_T (\nabla u_l + \nabla u_l^T)^2 - \rho_l C_{\varphi 2} \varphi^2 / k + \varphi / k C_\varphi S_k \quad (17)$$

where S_k is the additional source term comprehensive of turbulence induced by bubble:

$$S_k = -C_k \varepsilon_g \nabla p u_{\text{slip}} \quad (18)$$

The continuity equation for two phase systems is:

$$\partial / \partial t (\varepsilon_l \rho_l + \varepsilon_g \rho_g) + \nabla (\varepsilon_l \rho_l u_l + \varepsilon_g \rho_g u_g) = 0 \quad (19)$$

The momentum equation for gas phase:

$$(\partial \varepsilon_g \rho_g) / \partial t + \nabla (\varepsilon_g \rho_g u_g) = 0 \quad (20)$$

Invoking the equation of state for each phase:

$$\rho_l = \text{const.}, \rho_g = (M p)/(R T) \quad (21)$$

and following closure relation:

$$\varepsilon_l + \varepsilon_g = 1 \quad (22)$$

We obtain a closed system of ten differential and algebraic equations, which describes the dynamics of the two-phase flow and can be solved numerically when specific conditions are reached [33]. Solving of such system on relatively large computing domain needs nonstandard hardware or specific computing conditions (clusters for parallel computing).

Other option is provide initial calculation with simplified model. When low gas fraction occurs in the system, the value of ε_l is close to one. If we neglected the variation of ε_l due to the presence of gas in the continuity equation for the liquid phase eq. (19) becomes:

$$(\partial\varepsilon_l)/\partial t + \nabla(\varepsilon_l u_l) = 0 \quad (23)$$

It will be transformed into (with assumption $\varepsilon \approx 1$):

$$\nabla u_l = 0 \quad (24)$$

The gas velocity is then calculated as a sum of liquid velocity, slip velocity and drift velocity:

$$u_g = u_l + u_{slip} + u_{drift} \quad (25)$$

where the slip velocity u_{slip} is calculated by equation (9), and drift velocity u_{drift} is the additional condition for employed turbulent model, calculated as:

$$u_{drift} = -\eta_T/\square_l \nabla\varepsilon_g/\varepsilon_l \quad (26)$$

The continuity equation can be used for calculation local distribution of gas hold-up.

1.5.1. Boundary condition

2D axial symmetry was used. Gas input condition at the bottom is given as gas mass flux calculated as product of superficial gas velocity and effective density.

$$N_p = -n (\rho_g^* U_g) \quad (27)$$

where

$$\rho_g^* = \rho_g \varepsilon_g \quad (28)$$

$$U_g = Q_g/A_g \quad (29)$$

Gas outlet boundary condition is used in top, where the gas phase flows outward with the gas velocity - u_g . Condition for liquid at same position is treated as outlet with defined pressure. Boundary condition at left hand wall is axial symmetry.

Rests of boundaries are adjusted as walls with a no slip condition. There are generally two approaches for adjusting boundary conditions at solid walls implemented into commercial software. Both are using empirical models to calculate the thin laminar boundary layer adjacent to the solid walls. The first approach is “Wall offset”, the second is “Wall offset in viscous units”. More details can be found in user manual COMSOL. Wall offset setup has been used here.

Bubble diameters calculated by equation (10) and drag coefficients for contaminated systems (see Fig. 1) related for inlet gas volumetric flow are reported in Tab. 1.

Table 1. Bubble diameter and drag coefficient as function inlet gas volumetric flow

Q	d_b	c_D
[m ³ /s]	[mm]	[-]
1.11 * 10-04	5.8	2.30
1.67 * 10-04	6.8	2.46
2.22 * 10-04	7.7	2.58
2.78 * 10-04	8.4	2.67
3.33 * 10-04	9.0	2.75
3.89 * 10-04	9.6	2.81
4.44 * 10-04	10.1	2.87
5.00 * 10-04	10.6	2.91
5.56 * 10-04	11.1	2.96

1.5.2. Mesh grid

Triangular mesh elements were used for creating computational domain. Distance between the elements was 0.007 m. Distance between mesh elements at problematic places (both ends of draft tube) was 0.001 m.

1.5.3. Numerical Stabilization

Isotropic diffusion and streamline diffusion, or both can be added for the momentum equations as well as the gas transport equation. The momentum equation is stabilized using streamline diffusion by default. Gas transport equation is stabilized by default using both terms. Note, a suitable scale for the effective gas density and the bubble number density must be specified. More information about numerical stabilization is in the manual COMSOL.

1.5.4. Solving the model

Default element type: Lagrange – P₂P₁
 Analysis type: Transient
 Solver: Time dependent segregated
 Time stepping: time 0-60 second
 Relative tolerance 0.001
 Absolute tolerance 0.0001

Segregated groups:	1 – u_l , v_l (liquid velocity, radial and vertical component), p (pressure), ρ_{geff} (effective gas density) 2 – $\log k$ (logarithm of turbulent kinetic energy), $\log d$ (logarithm of turbulent dissipation rate)
Method:	BDF backward differentiation formulas (it uses variable-order variable-step-size)

2. Experimental

Schematic view of experimental apparatus is in Fig. 2. Pachuca tank is the name used for industry scale clone of such apparatus. It is typical equipment in hydrometallurgy for leaching of key component from ore. Our apparatus consist of glass vessel and has diameter of 15 cm and height of 150 cm. The draft tube is inside. Gas hold-up is measured by pressure difference in reverse U-tube manometer. A Pitot tube has been used for liquid velocity measurements. Geometry of draft tube is varied in length and diameter of draft tube (length of 0.8 and 0.6 m and diameter of 0.1, 0.08 and 0.06 m). The next geometrical variable has been distance of draft tube from bottom, which ranges from 15 mm to 65 mm.

In experiments has been used two-phase system air-water.

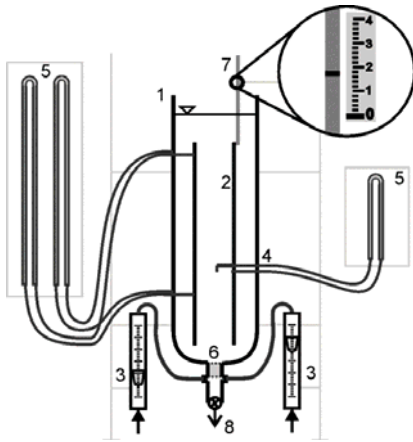


Fig. 2. Experimental apparatus; 1-Laboratory airlift reactor, 2-Draft tube, 3-Gas inlet and flow-meters, 4-Reverse U-tube manometer for measure pressure difference (to interpretation of gas hold-up), 5-Reverse U-tube manometer for measure liquid velocity by Pitot tube, 6-Gas bubbles distributor, 7-Reading distance of draft tube from bottom, 8-Escape valve;

Three types of experimental set-ups are reported here. The list of set-up parameters is given in Tab. 2. The distance between draft tube and bottom was calculated by:

$$h_B = 0.4 d_{\text{internal}} \quad (30)$$

Table 2. Geometry and position of draft tube in the experimental reactor

	h_B (m)	d_{internal} (m)	d_{external} (m)	$A_{\text{down}} / A_{\text{rise}}$ (1)	$h_{\text{draft tube}}$ (m)
type 1	0.02	0.052	0.06	7.05	0.8
type 2	0.03	0.072	0.08	3.07	0.8
type 3	0.035	0.092	0.10	1.49	0.8

Main measured quantity is pressure difference resulting to gas hold-up. The gas hold-up is defined as volume fraction of gas phase in the gas-liquid dispersion in the reactor.

$$\varepsilon_{gr,d} = \rho_l / (\rho_l - \rho_g) \Delta h_{r,d} / \Delta z_{r,d} \quad (31)$$

The value of liquid circulation velocity U_{lr} is one of the most important design parameter for airlifts or Pachuca reactors. Liquid circulation has influence on to the gas hold-up in the vessel, to heat and mass transfer coefficient and to the extent of mixing in the reactors [2]. The liquid velocity has been measured by Pitot tube. Pressure difference has been read from the inverse U-tube manometer:

$$U_{lr} = (2 g \rho_L \Delta h_r / \rho_{Dr})^{0.5} \quad (32)$$

Gas holdup and liquid circulation velocity have been calculated from the experimental data and results are discussed in the section Results.

3. Results and discussion

The model was constructed in the COMSOL Multiphysics 3.5a, it means draw geometry, set-up boundaries and variables, mesh grid and solver set-up. This model was exported to the Matlab and there was generated loop simulation for all gas input flux, bubbles diameters and drag coefficients. Post-processing of results and comparison between experimental data and numerical solutions has been carried out also in the Matlab. The values of liquid velocity and gas hold-up were calculated as integrated variables per volume of riser and downcomer:

$$U_l = (\int 2 \pi r u_l dU_l) / (\int dV), \quad \varepsilon_g = (\int 2 \pi r \varepsilon_g d\varepsilon_g) / (\int dV) \quad (33)$$

The main comparison between numerical solution and experimental data is figured out in following figures. The figures are dividing by results of liquid velocity in riser and gas hold-up in riser and in downcomer. These parameters have been plotted for gas volumetric flow and superficial gas velocity in the draft tube.

3.1. Liquid circulation velocity

The liquid velocity in riser increases with increasing gas volumetric flow. Influence of draft tube diameter on the liquid velocity in riser can be seen in Fig. 3. With decreasing diameter of draft tube the liquid velocity increases. Pretty good agreement of experiments and numerical simulations can be seen for prediction of liquid circulation velocity with increasing gas inlet volumetric flow

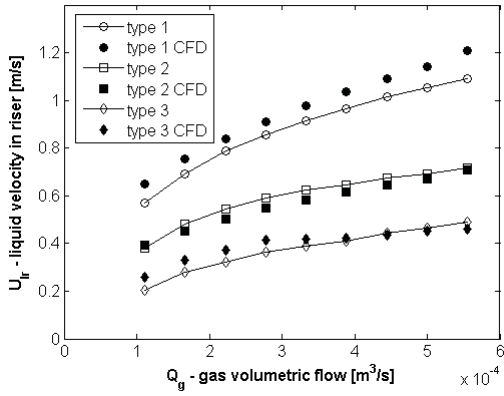


Fig. 3. Liquid velocity in riser as a function of gas volumetric flow for various diameter of draft tube

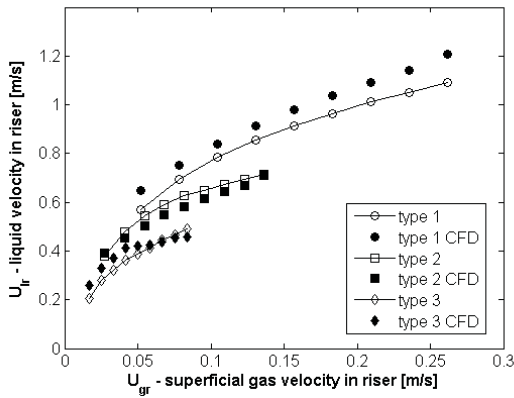


Fig. 4. Liquid velocity in riser as a function of superficial gas velocity in riser for various diameter of drat tube

3.2. Gas hold-up

Gas hold-up is one of important parameters of airlift reactors or bubble columns. Gas hold-up in reactor increases with increasing gas volumetric flow. Linear trend of gas hold-up in riser can be seen in Fig. 5. The difference between experimental data and CFD simulation has been caused by assumption of homogeneous distribution of bubble diameter in the reactor and neglecting of bubble coalescence, which corresponds with original setup of bubbly flow model build in COMSOL.

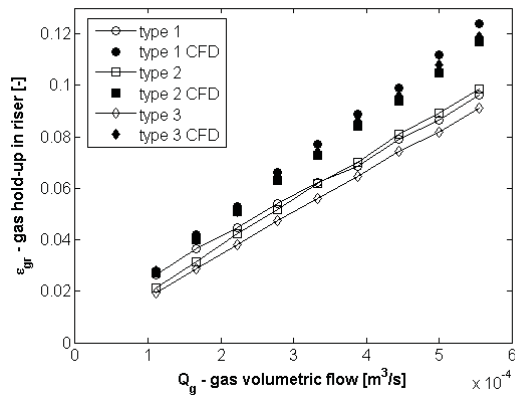


Fig. 5. Gas hold-up in riser as a function of gas volumetric flow for various diameter of draft tube

Heterogeneous and Slug bubbly flow regimes are main flow regimes which occurs during experiments carried out in our apparatus. In these regimes coalescence takes place and bubble sizes are not uniform. Homogeneous and transient and heterogeneous bubble flow regimes which are typical for bubble columns [33], did not occurs at our conditions.

In small draft tube diameters we have used, the Slug bubble flow regime is dominant, it means, that resulting bubbles produced by coalescence of initial bubbles are the same size as a diameter of draft tube. Such behavior was visually observed in our experiments.

The influence of diameter of draft tube on the gas hold-up in riser can be seen in Fig. 6. With increasing of draft tube diameter gas hold-up in riser decreases for same values of superficial gas velocity in riser.

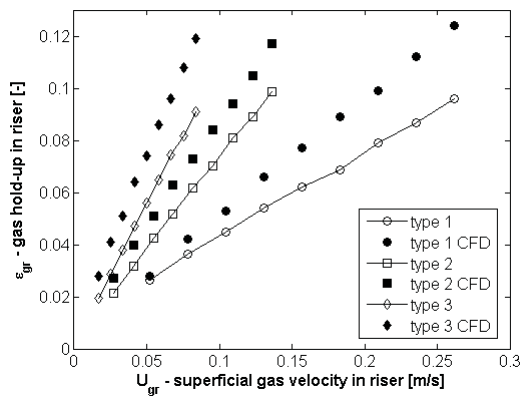


Fig. 6. Gas hold-up in riser as a function of superficial gas velocity in riser for various diameter of draft tube

Gas hold-up in downcomer increases with increasing gas volumetric flow. The influence of diameter of the draft tube to the gas hold-up in downcomer can be seen in Fig. 7, 8. Gas hold-up in downcomer increases with increasing of draft tube diameter for same values of inlet gas volumetric flow or superficial gas velocity. The differences between experiments and CFD simulation for higher values of gas

volumetric flow in geometry of type 2 and 3 are caused by total circulations of bubbles. The similar problem was described by van Benthum [4].

Smaller bubbles follow liquid stream and fall down through the downcomer. When the liquid circulation velocity in downcomer is high enough (more than 0.3 m/s) the total circulation of small bubbles is presented. The used model is not capable to correctly describe such behavior. On Fig. 8 can be seen small increasing of gas hold-up in downcomer for geometry of type 1 with increasing superficial gas velocity in riser. The total circulations of bubbles were not observed in experiments for this geometry.

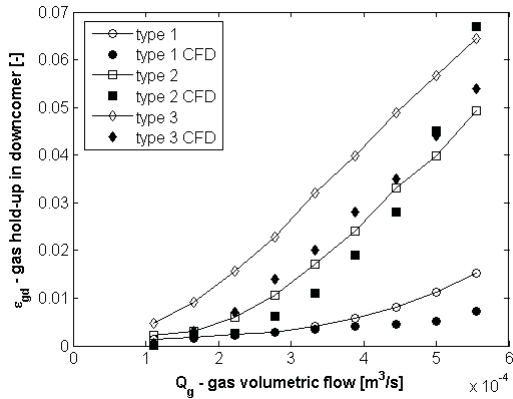


Fig. 7. Gas hold-up in downcomer as a function of gas volumetric flow for various diameter of drat tube

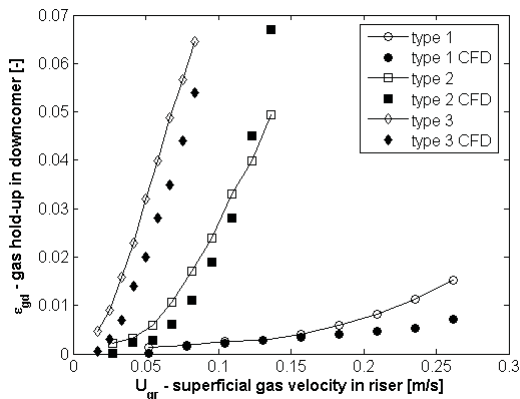


Fig. 8. Gas hold-up in downcomer as a function of superficial gas velocity in riser for various diameter of drat tube

4. Conclusions

Experimental investigation of geometrical parameters on to the two phase hydrodynamics effect in airlift reactor was carried out. Three different geometries of airlift with internal circulation loop were studied. Numerical simulation of experimental conditions using commercial software COMSOL was made. Experimental results and numerical simulations were compared when pretty good agreement (\pm)

10%) was found for prediction of gas holdup and liquid circulation velocity for small inlet gas volumetric flows and medium size and large draft tube. Data for high inlet volumetric flow and smaller draft tube are loaded by significant error. This is a task for no adequate simplification of numerical model, which, on the other hand, allow us to solve such complex problem with standard personal computer almost in real time.

Acknowledgements

The Generous support of this study by SP2012/196 and GAČR under projects 104/07/1110, 104/09/0972 is gratefully acknowledged.

References

- [1] Blenke H. Loop Reactors. *Adv Biochem Eng* 1979;**13**:122-213.
- [2] Chisti MY. *Airlift Bioreactors*. London: Elsevier Applied Science; 1989.
- [3] Heijnen JJ, Hols J, van der Lans RGJM, van Leeuwen HLJM. A simple hydrodynamics model for the liquid circulation velocity in full-scale two- and three-phase internal airlift reactor operating in the gas recirculation regime. *Chemical Engineering Science* 1997;**52**:2527-2540.
- [4] van Benthum WAJ, van der Lans RGJM, Heijnen JJ. Bubble circulation regimes in an internal-loop airlift reactor. *Chem Eng Sci* 1999;**54**:3995-4006.
- [5] Oey RS, Mudde RF, Portela LM. Simulation of a slurry airlift using a two-fluid model. *Chem Eng Sci* 2001;**56**:673-681.
- [6] van Baten JM, Ellenberer J, Krishna R. Using CFD to describe the hydrodynamics of internal air-lift reactors. *The Canadian J Chem Eng* 2003;**81**:660-668.
- [7] Oey RS, Mudde RF, van der Akker HEA. Numerical simulation of an oscillating internal-loop airlift reactor. *Can J Chem Eng* 2003;**81**:684-691.
- [8] Huang Q, Yang Ch, Yu G, Mao ZS. CFD simulation of hydrodynamics and mass transfer in an internal airlift loop reactor using a steady two-fluid model. *Chem Eng Sci* 2010;**65**:5527-5536.
- [9] Simcik M, Mota A, Ruzicka MC, Vicente A, Teixeira J. CFD simulation and experimental measurement of gas holdup and liquid interstitial velocity in internal loop airlift reactor. *Chem Eng Sci* 2011;**66**:3268-3279.
- [10] van der Lans RGJM. Hydrodynamics of a bubble column reactor. *PhD. thesis*. Delft; 1985.
- [11] Azzopardi BJ, Mudde RF, Morvan H, Yan YY, Zhao D. *Hydrodynamics of gas-liquid reactors: normal operation and upset condition*. 1st ed. John Wiley & Sons Ltd; 2011.
- [12] Sokolichin A, Eigenberger G. Gas-liquid flow in bubble columns and loop reactors: Part I. detailed modeling and numerical simulation. *Chem Eng Sci* 1994;**49**:5735-5746.
- [13] Becker S, Sokolichin A, Eigenberger G. Gas-liquid flow in bubble columns and loop reactors: Part II. comparison of detailed experiments and flow simulations. *Chem Eng Sci* 1994;**49**:5747-5762.
- [14] Schwarz MP, Turner WJ. Applicability of the standard k- ϵ turbulence model to gas-stirred baths. *Appl Math Model* 1988;**12**:273-279.
- [15] Cook TL, Harlow FH. Vortices in bubbly two-phase flow. *Int J Multiphase Flow* 1986;**12**:35-61.
- [16] Thomas NH, Auton TR, Sene K, Hunt JCR. Entrapment and transport of bubbles in transient large eddies in multiphase turbulent shear flow. *International conference on the physical modelling of multi-phase flow*, Coventry, UK, 1983:169-184.
- [17] Delnoij E, Kuipers JAM, van Swaaij WPM. A three dimensional CFD model for gas-liquid bubble columns. *Chem Eng Sci* 1999;**54**:2217-2226.
- [18] Boisson N, Marlin MR. Numerical prediction of two-phase flow in bubble columns. *Int J Num Methods Fluids* 1996;**23**:1289-1310.

- [19] Krishna R, Urseanu MI, van Baten JM, Ellenberger J. Influence of scale on the hydrodynamics of bubble columns operating in the churn-turbulent regime: experiments vs. Eulerian simulation. *Chem Eng Sci* 1999;**54**:4903-4911.
- [20] Deen NG, Solberg T, Hjertager BH. Numerical simulation of the gas-liquid flow in square cross-sectioned bubble column. *CHISA 14th Int. Congress of Chemical and Process Engineering*, Prague, CZE, 2000:16.
- [21] Mudde RF, van der Akker HEA., 2D and 3D simulation of an internal airlift loop reactor on the basis of a two-fluid model. *Chem Eng Sci* 2001;**56**:6351-6358.
- [22] Joshi JB. Computational flow modelling and design of bubble column reactors. *Chem Eng Sci* 2001;**56**:5893-5933.
- [23] Sokolichin A, Eigenberger G, Lapin A. Simulation of buoyancy driven bubble flow established simplification and open question. *AIChE J* 2004;**50**:24-45.
- [24] Bauer M, Eigenberger G. A concept for multi-scale modeling of bubble columns and loop reactors. *Chem Eng Sci* 1999;**54**:5109-5117.
- [25] Krishna R, van Baten JM, Urseanu MI, Ellenberger J. Design and scale up of a bubble column slurry reactor for Fisher-Tropsch synthesis, *Chem Eng Sci* 2001;**56**:537-545.
- [26] Johansen ST, Boysan F. Fluid dynamics in bubble stirred ladles: Part II. mathematical modelling. *Metal Trans B* 1988;**19B**:755-764.
- [27] Clift R, Grace JR, Weber ME. *Bubbles, Drops and Particles*. Dover Publication, Inc. New York; 1978.
- [28] Schiller L, Neumann A. A drag coefficient correlation. *VDI-Zeits* 1933;**77**:318-320.
- [29] Delnoij E, Kuipers JAM, van Swaaij WPM. Dynamics simulation of dispersed gas-liquid two-phase flow using a discrete bubble model. *Chem Eng Sci* 1997;**52**:3759-3772.
- [30] Ranade VV, van der Akker. A computational snapshot of gas-liquid flow in baffled stirred reactor. *Chem Eng Sci* 1994;**49**:5175-5192.
- [31] Bhanu C, Mazumdar D. Numerical prediction of melting rates in gas bubble driven systems. *Trans Indian Inst Met* 1997;**50**:249-258.
- [32] Prosperetti A, Tryggvason G. *Computational methods for multiphase flow*. Cambridge University Press. Cambridge; 2007.
- [33] Kastanek F, Sharp DH. *Chemical reactors for gas-liquid systems*. E. Horwood. Chichester; 1993.